A&A 411, L457–L460 (2003)
DOI: 10.1051/0004-6361:20031437

Astronomy & Astrophysics

Early SPI/INTEGRAL constraints on the morphology of the 511 keV line emission in the 4th galactic quadrant⋆

J. Knödlseder[1], V. Lonjou[1], P. Jean[1], M. Allain[1], P. Mandrou[1], J.-P. Roques[1], G. K. Skinner[1], G. Vedrenne[1], P. von Ballmoos[1], G. Weidenspointner[1,5], P. Caraveo[4], B. Cordier[3], V. Schönfelder[2], and B. J. Teegarden[5]

[1] Centre d'Étude Spatiale des Rayonnements, CNRS/UPS, BP 4346, 31028 Toulouse Cedex 4, France
[2] Max-Planck-Institut für Extraterrestrische Physic, Postfach 1603, 85740 Garching, Germany
[3] DSM/DAPNIA/SAp, CEA-Saclay, 91191 Gif-sur-Yvette, France
[4] IASF, via Bassini 15, 20133 Milano, Italy
[5] Laboratory for High Energy Astrophysics, NASA/Goddard Space Flight Center, Greenbelt, MD 20771, USA

Received 21 July 2003 / Accepted 16 September 2003

Abstract. We provide first constraints on the morphology of the 511 keV line emission from the galactic centre region on basis of data taken with the spectrometer SPI on the INTEGRAL gamma-ray observatory. The data suggest an azimuthally symmetric galactic bulge component with *FWHM* of ∼9° with a 2σ uncertainty range covering 6°−18°. The 511 keV line flux in the bulge component amounts to $9.9^{+4.7}_{-2.1} \times 10^{-4}$ ph cm^{-2} s^{-1}. No evidence for a galactic disk component has been found so far; upper 2σ flux limits in the range $(1.4-3.4) \times 10^{-3}$ ph cm^{-2} s^{-1} have been obtained that depend on the assumed disk morphology. These limits correspond to lower limits on the bulge-to-disk ratio of 0.3−0.6.

Key words. gamma rays: observations

1. Introduction

Since the first detection (Johnson & Haymes 1973) and the subsequent identification (Leventhal et al. 1978) of the galactic 511 keV annihilation line, the origin of galactic positrons has become a lively topic of scientific debate. Among the proposed source candidates figure compact objects such as neutron stars or black holes (Lingenfelter & Ramaty 1983), stars, such as supernovae, novae, red giants and Wolf-Rayet stars, expelling radioactive nuclei produced by nucleosynthesis (Ramaty et al. 1979), cosmic-ray interactions with the interstellar medium (Kozlovsky et al. 1987), pulsars (Sturrock 1971), gamma-ray bursts (Lingenfelter & Hueter 1984) and stellar flares. Yet so far the source of the galactic positrons is still unknown.

The question of the morphology of the galactic 511 keV annihilation signal is intimately related to the question of the origin of galactic positrons. The celestial distributions should be tied to the source distribution, although positron diffusion within the Galaxy may to some extent blur this link. Although earlier measurements already provided first indications of the morphology of the emission (e.g. Share et al. 1990), it is only with the advent of the OSSE telescope onboard the Compton Gamma-Ray Observatory that a first crude skymap of the 511 keV intensity distribution became available (Cheng et al. 1997; Purcell et al. 1997; Milne et al. 2000, 2001). The OSSE observations suggest at least two emission components, one being a spheroidal bulge and the other being a galactic disk component. Indications of a third component situated above the galactic plane have resulted in various speculations about the underlying source (von Ballmoos et al. 2003), yet the morphology and intensity of this component is only poorly determined (e.g. Milne et al. 2001).

Modelling the bulge component by symmetric gaussians, the OSSE data suggest *FWHM* values in the range 4°−6° with no significant offset from the galactic centre (Purcell et al. 1997; Milne et al. 2000). TGRS results are also consistent with no significant offset from the centre ($\lesssim$2°) but suggest a somewhat broader distribution (Harris et al. 1998). The estimated bulge-to-disk ratio (hereafter B/D ratio) is only poorly constrained by the observations, and estimates vary from 0.2−3.3 depending upon whether the bulge component features a halo (which leads to a large B/D ratio) or not. The total flux has been constrained to $(2.1-3.1) \times 10^{-3}$ ph cm^{-2} s^{-1} (Milne et al. 2000).

Clearly, more observations are needed to better constrain the 511 keV emission morphology, and thus to shed light on the origin of galactic positrons. In this paper we report a step towards this direction by exploiting a first set of data recorded

Send offprint requests to: J. Knödlseder,
e-mail: knodlseder@cesr.fr

⋆ Based on observations with INTEGRAL, an ESA project with instruments and science data centre funded by ESA member states (especially the PI countries: Denmark, France, Germany, Italy, Switzerland, Spain), Czech Republic and Poland, and with the participation of Russia and the USA.

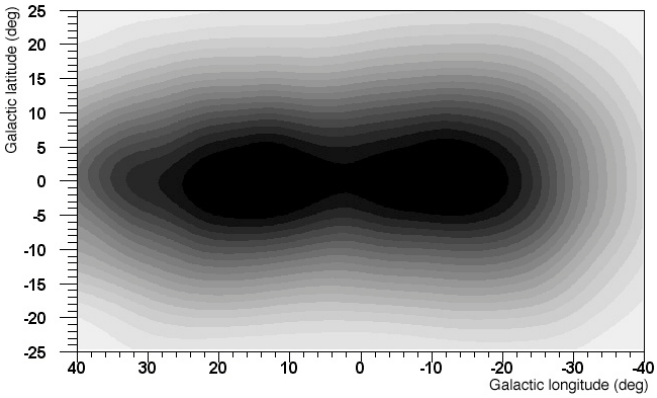

Fig. 1. Relative exposure map of the galactic centre region. Black corresponds to regions of maximum exposure.

by the spectrometer SPI on ESA's INTEGRAL observatory. First results on the spectral shape of the 511 keV line obtained from the same set of data, indicating a slightly broadened line of $2.95^{+0.45}_{-0.51}$ keV *FWHM*, have been reported elsewhere (Jean et al. 2003).

2. Data analysis

The data analysed in this work were accumulated during the first year's Galactic Centre Deep Exposure (GCDE) and Galactic Plane Scan (GPS), executed as part of INTEGRAL's guaranteed time observations (see Winkler 2001). We used data from 19 orbits from March 3rd to April 30th, 2003, amounting to a total effective exposure time of 1667 ks. The GCDE consists of rectangular pointing grids covering galactic longitudes $l = \pm 30°$ and latitudes $b = \pm 10°$, with reduced exposure up to $b = \pm 20°$. The GPS consists of pointings within the band $b = \pm 6.4°$ along the galactic plane. For details see Winkler (2001). The present data are from 1199 pointings with an average exposure of 1400 s per pointing.

As a result of data sharing agreements, the results presented here are limited to the galactic quadrant $l = 270°-360°$ but, in accordance with those agreements, data from pointings in the entire GCDE region $l = \pm 30°$ have been taken into account in the analysis. The resulting sky exposure is depicted in Fig. 1, where black/white corresponds to regions of maximum/minimum exposure, respectively. A quite homogeneous exposure has been achieved over galactic longitudes $\pm 25°$, with a small exposure dip near the galactic centre. The latitude dependence is approximated by a Gaussian centred on the galactic plane, with *FWHM* of $\sim 30°$.

Data preparation and modelling of the instrumental background is identical to that described in Jean et al. (2003). The SPI single detector event data have been gain corrected and binned into event spectra of 0.25 keV bin width for each detector and pointing, leading to a 3-dimensional data space. The background has been modelled in this data space by two components, accounting for the instrumental 511 keV line and the underlying continuum (see Eqs. (1) and (2) and Fig. 1 in Jean et al. 2003). The short-term variability (<3 days) of the background has been predicted using the rate of saturating events in the Ge detectors, while the long-term variability has been regarded as an unknown (see Sect. 4).

The expected number of counts in this data space, $E_{\mathrm{p,d,e}}$, where "p" indicates the pointing, "d" the detector, and "e" the energy bin, is given by

$$E_{\mathrm{p,d,e}} = \sum_{l,b} R^{l,b}_{\mathrm{p,d,e}} \Phi_{l,b} + B_{\mathrm{p,d,e}}, \quad (1)$$

where $R^{l,b}_{\mathrm{p,d,e}}$ is the instrumental response matrix (i.e. the number of counts in a data space bin that arises from a source of unit flux at the sky position l, b; see Sturner et al. 2003), $\Phi_{l,b}$ is the 511 keV sky intensity distribution, and $B_{\mathrm{p,d,e}}$ is the background model. In the following we describe two approaches that we used to extract information about $\Phi_{l,b}$ from the measured SPI data.

3. Imaging

A qualitative impression about the spatial distribution of the 511 keV γ-ray line emission can be obtained by deconvolving the data into a celestial intensity distribution. For this purpose, we employed in this work the Richardson-Lucy algorithm (Richardson 1972; Lucy 1974) that has been successfully applied to γ-ray data of earlier missions (e.g. Knödlseder et al. 1999; Milne et al. 2000). The Richardson-Lucy algorithm decomposes the sky into a grid of equally sized pixels (here of $0.5° \times 0.5°$) and solves for the intensity $\Phi_{l,b}$ in each of the pixels simultaneously using an iterative maximum likelihood scheme. The pixels are constrained to positive intensities. As all pixel-based deconvolution algorithms, the Richardson-Lucy scheme leads to morphology artefacts in the case of reconstructing a diffuse low significance signal since the number of free parameters (i.e. the number of image pixels) greatly exceeds the information available in the data. In order to reduce these artefacts, we added a smoothing step to the iterative scheme that effectively combines adjacent pixels and thus reduces the number of pixels in the reconstruction. As smoothing kernel, a boxcar average of $6° \times 6°$ has been employed.

Figure 2 shows the resulting skymap for negative longitudes (according to the above cited data right agreements we deliberately limit the image to $l < 0°$). As insets, longitude and latitude profiles of the 511 keV line emission are shown that have been obtained by integrating the intensity of latitudes $b = \pm 5$ deg and longitude $l = -5°-0°$, respectively. The emission is concentrated in an azimuthally symmetric region near the galactic centre, with an extent of about $\sim 9°$ (*FWHM*). The emission maximum is slightly offset from the galactic centre, and is situated at about $l = -1°$ and $b = 2°$. Integrating the intensity over the feature suggests a flux of the order of 10^{-3} ph cm^{-2} s^{-1}.

To asses the significance of the morphology that is seen in the skymap, we performed Monte-Carlo simulations of the deconvolution process assuming that the 511 keV line emission morphology is described by an azimuthally symmetric Gaussian bulge of $10°$ *FWHM* centred at $l = 0°$ and $b = 0°$. In the ideal case the image deconvolution should reproduce the input image of an azimuthally symmetric emission centred at the

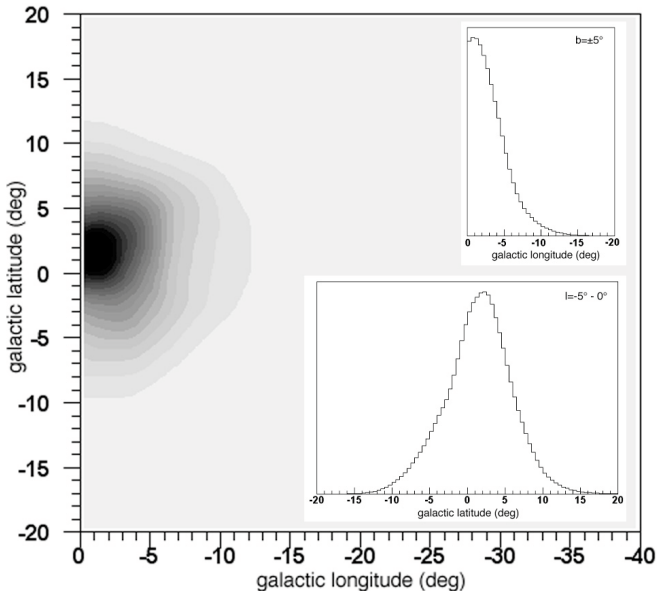

Fig. 2. 511 keV gamma-ray line intensity map of the galactic centre region (only negative longitudes). Black corresponds to regions of maximum 511 keV line intensity. Longitude and latitude profiles, integrated over $b = \pm 5^\circ$ and $l = -5^\circ - 0^\circ$, respectively, are shown as insets.

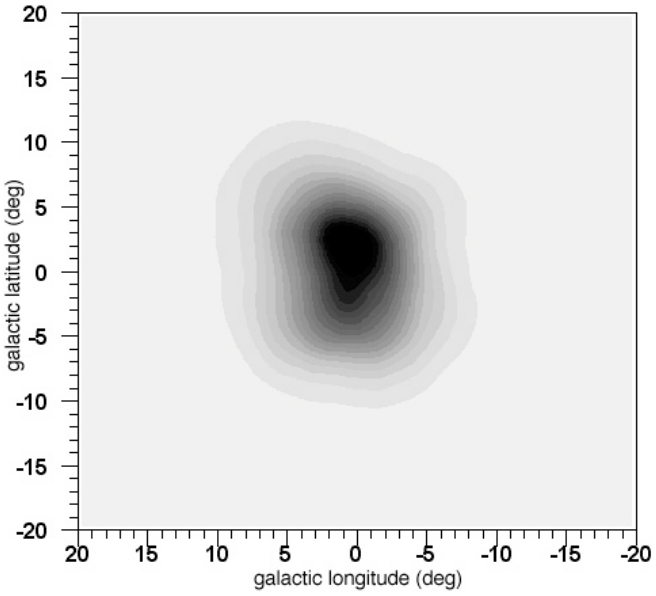

Fig. 3. Simulated 511 keV gamma-ray line intensity map based on an azimuthally symmetric Gaussian model of 10° *FWHM* centred at $l = 0^\circ$ and $b = 0^\circ$.

galactic centre, yet the limited statistics may introduce some uncertainties in the reconstruction procedure.

Figure 3 shows the resulting simulated skymap, now shown for the entire galactic centre region. Obviously, although the underlying model has been azimuthally symmetric, the deconvolved image shows a clear emission asymmetry, with *FWHM* of 8° and 12° in the longitudinal and latitudinal directions, respectively. Also the emission maximum is displaced from the galactic centre, and is found at $l = 0.5^\circ$ and $b = 2.5^\circ$. These values are comparable to those found for the centroid of the emission in the 511 keV sky map, and as we will show more quantitatively in the next section, the apparent displacement in the 511 keV sky map could indeed be of purely statistical nature.

4. Model fitting

A more quantitative approach is possible by fitting to the data a model of the spatial distribution that has one or more components. The components can be point sources, Gaussian or other geometric forms, or arbitrary maps corresponding to known distributions. The intensities of the components are adjusted to maximise the likelihood that the model gives rise to the observed distribution of counts in the line (a 5 keV wide energy band centred at 511 keV was used), binned by detector and by pointing. Along with the model intensities, 19 background model scaling factors have been adjusted for the line component by the fit, one for each orbit (factors G in Jean et al. 2003); the scaling factors for the continuum component (factors F in Jean et al. 2003) have been fixed to unity. Not fitting the background model introduces systematic uncertainties in the analysis that considerable biases the morphology determination.

Guided by the imaging analysis (and by previous work performed to describe the morphology of the OSSE observations, e.g. Purcell et al. 1997) we used Gaussian functions to describe the observed bulge emission. Assuming an azimuthally symmetric Gaussian centred on $l = 0^\circ$ and $b = 0^\circ$ results in an optimum *FWHM* of 9^{+7}_{-3} degrees, where the quoted uncertainties are formal statistical 2σ errors. Systematic uncertainties, due to different treatment of the instrumental background, hardly affect the lower boundary, while adding an additional uncertainty of $\pm 2^\circ$ to the upper boundary. The flux in the bulge component amounts to $9.9^{+4.7}_{-2.1} \times 10^{-4}$ ph cm^{-2} s^{-1}, where the uncertainty includes (and is dominated by) the uncertainty in the Gaussian width. Formally, the statistical detection significance of the 511 keV line amounts to 12σ.

Relaxing the condition on spherical symmetry does not significantly improve the fit. Yet relaxing the condition on the location of the bulge centroid improves the likelihood by 3.3 corresponding to a significance of 2.1σ for the displacement. The optimum centroid positions has been determined as to be $l = -1.0^\circ \pm 1.3^\circ$ and $b = 1.4^\circ \pm 1.3^\circ$, the optimum Gaussian width at this location amounts to 8^{+4}_{-3} degrees (2σ statistical errors). Systematic uncertainties in the centroid determination amount to about $\pm 0.2^\circ$. The flux in the displaced bulge component amounts to $10.3^{+2.6}_{-2.2} \times 10^{-4}$ ph cm^{-2} s^{-1}, including again the uncertainty in the Gaussian width.

Including a galactic disk component in addition to the Gaussian bulge component does not significantly improve the fit. In none of the considered cases did the fit attribute a significant flux to the disk component. From the fits we derive upper limits on the disk flux by multiplying the statistical uncertainty in the disk component by the requested significance level (we quote here 2σ upper limits, hence the formal 1σ statistical errors have been multiplied by a factor of 2). Although the disk models we tested formally cover the entire galactic plane,

the effective exposure of our data is restricted to $l \approx \pm 40°$, and hence we can only derive conclusions about this longitude range. For the bulge component we used an azimuthally symmetric Gaussian centred on $l = 0°$ and $b = 0°$ with the width being a free parameter of the fit. In all considered cases, the best fitting *FWHM* amounted to ∼9°, with a 2σ lower limit of 6°.

The resulting limits on the disk flux strongly depend on the spatial distribution that has been assumed for the disk component. Using models of constant positron annihilation surface density throughout the galactic disk, limited to a maximum galactocentric radius of 14 kpc, provide the largest upper flux limits, comprised between $(2.8–3.4) \times 10^{-3}$ ph cm^{-2} s^{-1} for assumed exponential scale heights of 90 and 325 pc, respectively. A tracer of the old stellar population, such as the DIRBE 35 μm allsky map, gives a slightly smaller limit of 2.5×10^{-3} ph cm^{-2} s^{-1}, while a massive star tracer, such as the DIRBE 240 μm allsky map, provides a considerably smaller limit of 1.4×10^{-3} ph cm^{-2} s^{-1}.

5. Discussion

The 511 keV line emission detected by SPI from the Galaxy is so far adequately described by a Gaussian shaped bulge of ∼9° *FWHM*. The 2σ lower limit on the bulge size amounts to 6°, which is at the upper limit of the values suggested by the OSSE observations (4°−6°). At this early stage of the analysis we do not emphasise this discrepancy, yet it may be taken as a first hint of morphology differences between the OSSE and SPI analyses.

The data do not suggest that the bulge geometry deviates from spherical symmetry yet a small offset of the centroid from the galactic centre direction is indicated by the data at the $\sim 2\sigma$ confidence limit. The present data do not yet allow to make a statement about the reality of the positive latitude enhancement that has been reported by Purcell et al. (1997).

Assuming that the bulge is indeed located at the galactic centre, at a distance of 8.5 kpc, the measured 511 keV line flux converts into an annihilation rate of $(3.4–6.3) \times 10^{42}$ s^{-1}. The observed flux is compatible with previous measurements that have been obtained using telescopes with small or moderate fields-of-view, yet it is on the low side when compared to OSSE measurements. OSSE, however, has detected an additional galactic disk component that is (so far?) not seen in the SPI data. The disk flux determined by OSSE lies in the range $(0.7–2.7) \times 10^{-3}$ ph cm^{-2} s^{-1}, and strongly depends on the assumed shape of the bulge component. Our 2σ upper limits on the disk component of $(1.4–3.4) \times 10^{-3}$ ph cm^{-2} s^{-1} are still compatible with the OSSE measurements.

The upper flux limits on the galactic disk component may be converted into lower limits for the bulge-to-disk ratio. While the constant surface density models provide the smallest limits of $B/D \geq 0.3$, the DIRBE 35 μm and 240 μm maps lead to $B/D \geq 0.4$ and $B/D \geq 0.6$, respectively. We included in these limits the 2σ uncertainty about the bulge size which translates into a typical uncertainty of 0.2 in the bulge-to-disk ratio. Again, these limits are compatible with the OSSE measurement of values in the 0.2−3.3 range.

6. Conclusions

The analysis of SPI data that have been recorded during the first half of the first year's INTEGRAL GCDE have provided initial constraints on the morphology of the galactic 511 keV line emission. The data suggest that the emission follows an azimuthally symmetric galactic bulge of ∼9° typical *FWHM*, yet the uncertainties on the width are still rather large (6°−18°, 2σ). The bulge seems centred on the galactic centre, yet a marginal displacement towards positive latitudes and negative longitudes may be indicated. Obviously, this displacement clearly needs confirmation by the analysis of a much larger set of data.

The available SPI observations are so far rather insensitive to a galactic disk component, and only upper limits have been derived. More data along the galactic plane are needed to better constrain the disk component. These data are, to some extent, already taken, yet the data sharing agreements do not allow for their inclusion in the present analysis. Yet we are optimistic that once combined, the complete set of SPI observation will provide unprecedented constraints on the morphology of the 511 keV line emission, and thus give us key information about the origin of the positrons in the Galaxy.

Acknowledgements. The SPI project has been completed under the responsibility and leadership of CNES. We are grateful to ASI, CEA, CNES, DLR, ESA, INTA, NASA and OSTC for support.

References

Cheng, L. X., Leventhal, M., Smith, D. M., et al. 1997, ApJ, 481, L43
Harris, M. J., Teegarden, B. J., Cline, T. L., et al. 1998, ApJ, 501, L55
Jean, P., Knödlseder, J., Lonjou, V., et al. 2003, A&A, 407, L55
Johnson, W. N., & Haymes, R. C. 1973, ApJ, 184, 103
Knödlseder, J., Dixon, D., Bennett, K., et al. 1999, A&A, 345, 813
Kozlovsky, B., Lingenfelter, R. E., & Ramaty, R. 1987, ApJ, 316, 801
Leventhal, M., MacCallum, C. J., & Stang, P. D. 1978, ApJ, 225, L11
Lingenfelter, R. E., & Hueter, G. J. 1984, in High-Energy Transients in Astrophysics, ed. S.E. Woosley, AIP Conf. Proc., 558
Lingenfelter, R. E., & Ramaty, R. 1983, in Positron-Electron Pairs in Astrophysics, ed. M. L. Burns, A. K. Harding, & R. Ramaty, AIP Conf. Proc., 267
Lucy, L. B. 1974, AJ, 79, 745
Milne, P. A., Kurfess, J. D., Kinzer, R. L., Leising, M. D., & Dixon, D. D. 2000, AIP Conf. Proc., 510, 21
Milne, P. A., Kurfess, J. D., Kinzer, R. L., & Leising, M. D. 2001, AIP Conf. Proc., 587, 11
Purcell, W. R., Cheng, L.-X., Dixon, D. D., et al. 1997, ApJ, 491, 725
Ramaty, R., Kozlovsky, B., & Lingenfelter, R. E. 1979, ApJS, 40, 487
Richardson, W. H. 1972, J. Opt. Soc. Am., 62, 55
Share, G. H., Leising, M. D., Messina, D. C., & Purcell, W. R. 1990, ApJ, 358, L45
Sturner, S. J., Shrader, C. R., Weidenspointner, G., et al. 2003, A&A, 411, L81
Sturrock, P. A. 1971, ApJ, 164, 529
Von Ballmoos, P., Guessoum, N., Jean, P., & Knödlseder, J. 2003, A&A, 397, 635
Winkler, C. 2001, Proc. 4th INTEGRAL workshop, ed. A. Gimenez, V. Reglero, & C. Winkler, ESA SP-459, 471